

# Ultrafast and reversible control of the exchange interaction in Mott insulators

J. H. Mentink,\* K. Balzer, and M. Eckstein

Max Planck Research Department for Structural Dynamics,  
University of Hamburg-CFEL, 22761 Hamburg, Germany

(Dated: May 30, 2023)

The strongest interaction between microscopic spins in magnetic materials is the exchange interaction  $J_{\text{ex}}$ . Therefore, ultrafast control of  $J_{\text{ex}}$  keeps the promise to control spins on ultimately fast timescales. We demonstrate that time-periodic modulation of the electronic structure by sub-picosecond laser pulses can be used to reversibly control the exchange interaction on ultrafast timescales in extended Mott insulators. In the regime of weak-driving strength relevant for condensed matter systems, we find that the exchange interaction can be enhanced and reduced for frequencies below and above gap, respectively. For strong driving strength, which might be achieved in cold-atom systems, even the sign of the exchange interaction can be reversed. We show that this causes time reversal of the associated quantum spin dynamics, which opens up possibilities for fundamental studies concerning the reversibility of the quantum many-body dynamics.

Controlling magnetically ordered systems on sub-picosecond timescales is currently a widely studied research area owing to the joint fundamental interest and technological demand for faster and more energy-efficient magnetic storage [1]. The fastest pathways to reverse magnetic order utilize the exchange interaction  $J_{\text{ex}}$  between microscopic magnetic moments [2–6], which can exceed external magnetic fields by orders of magnitude. Because  $J_{\text{ex}}$  relies on the electrostatic Coulomb repulsion and the Pauli principle rather than on magnetic dipole forces, it may be modified directly by the action of a laser pulse on the electronic state. This implies an appealing and largely unexplored scenario to control magnetism on the fastest possible timescale. Recently, several studies have discussed an ultrafast modification of  $J_{\text{ex}}$  by creating a nonequilibrium electron distribution (by photo-doping or laser-heating) [7–15]. In these cases the spin dynamics after the excitation strongly depends on the relaxation of the electrons, thereby hindering a direct and reversible control of the spin degrees of freedom alone. On the other hand, reversible electrical control of  $J_{\text{ex}}$  was recently demonstrated in a multiferroic solid state system, where the bond alignment can be changed by a static electric field [16]. Clearly, a natural goal is to achieve control of  $J_{\text{ex}}$  which is both reversible *and* ultrafast, *i.e.*, it is active while a laser pulse is on, but leaves the electronic state unexcited after the pulse is switched off. As we will demonstrate, this is possible by periodically modulating the electronic structure with a frequency  $\omega$  higher than  $J_{\text{ex}}/\hbar$ , but not resonant to electronic excitations.

The use of periodic driving to control the dynamics of a quantum system is known in many areas of physics, *e.g.*, through effective conservative forces resulting from the AC Stark effect, or through the coherent destruction of tunneling [17, 18]. The idea of designing an effective low-energy spin Hamiltonian by periodic driving was pioneered for ultra-cold bosons [19], in a double-well system

driven near resonant to an externally induced splitting of the two lowest levels. In this paper we investigate how effectively and how reversibly  $J_{\text{ex}}$  can be controlled in *extended* fermionic lattice systems, by looking at a simple driving scheme using time-periodic electric fields. This scheme can be realized both in solid state systems and for cold atoms, which suggests wide applications: Besides the possibility of manipulating magnetism in solids, *e.g.*, via the excitation of spin resonances, we find that in the extreme limit of strong driving one may even achieve a sign reversal of  $J_{\text{ex}}$ , which is equivalent of letting the system evolve backwards in time and may allow for addressing fundamental questions concerning the reversibility of quantum many-body dynamics [20–22] in cold atom experiments.

Particles in a tight-binding band subject to time-periodic electric fields or a periodic modulation of the hopping amplitude evolve under an effective Hamiltonian that has a different band structure [17, 18, 23–26]. While this band renormalization is certainly relevant for controlling  $J_{\text{ex}}$ , it will turn out to be more important how periodic driving influences the electronic correlations. In the Mott insulators that we will consider below, these effects can even dominate when  $\hbar\omega$  is comparable to the gap (but still large compared to the energy scale  $J_{\text{ex}}$ ) since it is the virtual charge excitations that determine the exchange interaction without driving. In this case, understanding the effect of periodic driving on the exchange interactions requires the solution of a strongly time-dependent many-body problem on a lattice.

We will show that considerable insight can be obtained from analytical Floquet theory for a few-site cluster under continuous driving, which predicts reversible enhancement, reduction and even complete sign-change of the exchange interaction. The relevance of these results for extended many-body systems may not be clear *a priori*, since in this case a true quasi-steady driven state may always become infinitely excited [27]. For the relatively short-term dynamics of interest here, the predictions of Floquet theory are nevertheless correct, as we demonstrate using numerical calculations for both the

\* Johan.Mentink@mpsd.cfel.de

classical spin dynamics in high-dimensional Mott insulators and the quantum spin dynamics in low-dimensional Mott insulators.

## I. RESULTS

In this work we study the repulsive Hubbard model as a paradigm model for strongly interacting electrons on a lattice. The Hamiltonian is given by

$$H = -t_0 \sum_{\langle ij \rangle \sigma} c_{i\sigma}^\dagger c_{j\sigma} + U \sum_j n_{j\uparrow} n_{j\downarrow}, \quad (1)$$

where  $c_{i\sigma}^\dagger$  creates an electron at site  $i$  with spin  $\sigma = \uparrow, \downarrow$ ,  $t_0$  is the hopping between nearest-neighbor sites, and  $U$  the repulsive on-site interaction. Arbitrary time-dependent electric fields  $\mathbf{E}(t)$  are incorporated by adding a Peierls phase to the hopping matrix elements (see Methods). Below we set  $\hbar = 1$  and measure energy and time in units of the hopping  $t_0$  and the inverse hopping, respectively. Electric fields are measured in units of  $t_0/ea$ , where  $a$  is the lattice spacing and  $e$  the electron charge.

For half-filling and  $U/t_0 \gg 1$ , the Hubbard model describes a Mott insulator with one electron per site, in which the remaining spin degrees of freedom are coupled by an antiferromagnetic exchange interaction  $J_{\text{ex}} = 2t_0^2/U$ . The simplest analytical understanding for this result is obtained already for two electrons on two Hubbard sites: Among the four states (for total  $S_z = 0$ ) there are two states with high energies close to  $U$ , involving a charge transfer excitation, as well as the singlet and triplet states with one electron per site and energies  $E_S = -4t_0^2/U$  and  $E_T = 0$ , respectively. The low-energy spectrum is thus described by a spin Hamiltonian  $2J_{\text{ex}}\mathbf{S}_1\mathbf{S}_2$  with  $J_{\text{ex}} = (E_T - E_S)/2 = 2t_0^2/U$ . This analytical understanding from the cluster is useful since lattice effects beyond the lowest-order perturbative result only appear in the order  $t_0^4/U^3$ . In the same spirit, to gain theoretical insight into the modification of  $J_{\text{ex}}$  by periodic driving, we first consider the same two-site Hubbard cluster and employ Floquet's theorem [28, 29], the analog of Bloch's theorem in time. When the Hamiltonian is periodic in time with a period  $T = 2\pi/\omega$ , solutions of the time-dependent Schrödinger equation are given in the form  $|\psi(t)\rangle = e^{-i\epsilon_\alpha t}|\psi_\alpha(t)\rangle$  where  $|\psi_\alpha(t+T)\rangle = |\psi_\alpha(t)\rangle$  is time-periodic, and  $\epsilon_\alpha$  is a quasi-energy defined up to multiples of  $\omega$ . The Floquet picture describes a system that undergoes virtual absorption and emission of an arbitrary number of photons, as depicted in Fig. 1c for the Mott-Hubbard systems. The unperturbed Floquet sectors are described by the time-averaged Hamiltonian shifted by  $n\omega$ , and mixing between these Floquet sectors results in a renormalization of quasi-energy levels. A natural procedure is then to adopt an "adiabatic" principle in which the driving amplitude varies slowly as compared to the driving frequency,  $|\dot{E}/E| \ll \omega$ , and identify the amplitude-dependent singlet-triplet splitting  $\epsilon_T - \epsilon_S$

in the quasi-energy spectrum with the (time-dependent) exchange interaction that describes the spin dynamics in the laser driven system on timescales much slower than the driving period  $T$ .

The numerical solution of the Floquet spectrum and various analytically tractable limiting cases for the two-site Hubbard model are detailed in the methods section. For a tight-binding model driven by an electric field  $E(t) = E_0 \cos(\omega t)$ , the coupling between Floquet sectors is controlled by the dimensionless Floquet amplitude

$$\mathcal{E} = \frac{eaE_0}{\hbar\omega}, \quad (2)$$

and the time-averaging of  $H$  corresponds to a coherent reduction of the tunneling amplitude [17, 18] by a factor  $J_0(\mathcal{E})$ , where  $J_0$  is the Bessel function (see Methods). In Fig. 1, we display the Floquet spectrum and the exchange splitting  $J_{\text{ex}}(\mathcal{E})$  for a half-filled two-site Hubbard model. In contrast to the limit  $\omega \gg U, t_0$ , where the only effect would be a renormalization of the hopping by  $J_0(\mathcal{E})$  and a corresponding reduction of the exchange splitting at large  $U$  by a factor  $J_0(\mathcal{E})^2$ , one can see that  $J_{\text{ex}}$  can be both increased and decreased for finite  $\omega$ , depending on the driving. This is clear already in the perturbative limit for  $\mathcal{E} \ll 1$  and  $t_0/U \ll 1$ , which is given by  $J_{\text{ex}} = 2t_0^2/U + \Delta J_{\text{ex}}$  with (see Methods)

$$\Delta J_{\text{ex}} = \frac{\mathcal{E}^2 t_0^2}{4} \left( \frac{1}{U + \omega} + \frac{1}{U - \omega} - \frac{2}{U} \right), \quad (3)$$

and indicated with (dash-)dotted lines in the right panel of Fig. 1. The last term of Eq. (3) is the reduction of the exchange due to coherent reduction of the tunneling, while the first two terms derive from the coupling to the  $m = \pm 1$  Floquet sector with effectively shifted charge transfer energies  $U \pm \omega$ . The net effect is an enhancement (reduction) of  $J_{\text{ex}}$  for driving frequencies below (above) the Coulomb energy  $U$ . For sufficiently strong driving one can even reverse the sign of  $J_{\text{ex}}$ , thus leading to the remarkable finding of a ferromagnetic exchange coupling in the half-filled Hubbard model. This happens when  $\mathcal{E}$  is of order one, such that coupling to higher Floquet sectors with effective Coulomb energy  $U - m\omega$  becomes strongly enhanced, while the direct exchange path is reduced by coherent destruction of tunneling  $\sim J_0(\mathcal{E})$ . For larger Floquet amplitudes, the direct exchange path again increases due to the oscillating behavior of the Bessel function. In the remainder of this paper we verify that these predictions from the two-site Floquet picture remain valid for extended condensed matter systems, in spite of the possible importance of absorption and of higher-order hopping processes.

**High-D lattice: mean-field spin dynamics** – A direct prediction of the Floquet theory (Eq. (3)) is the enhancement (reduction) of the exchange interaction for driving below (above) gap with weak amplitudes ( $\mathcal{E} \ll 1$ ). A large class of materials for which this might be relevant are three-dimensional bulk systems, such as transition metal oxides, whose low-energy spin dynamics con-

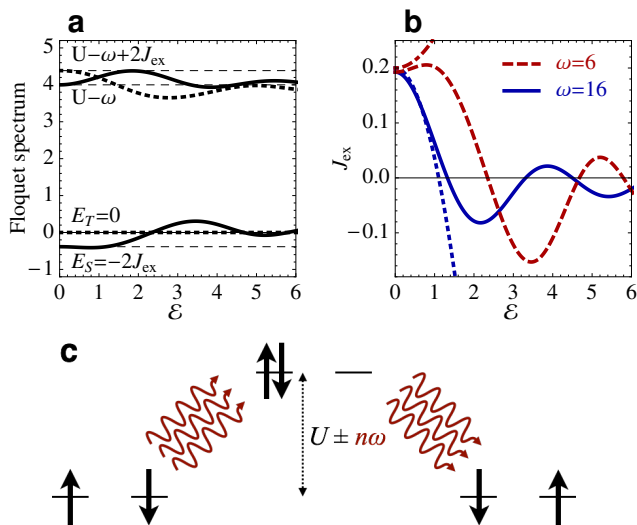


FIG. 1. **Floquet spectrum and extracted exchange interaction  $J_{\text{ex}}$  in a two-site Hubbard model.** (a) Floquet spectrum for  $U = 10$  and  $\omega = 6$ . The extracted  $J_{\text{ex}}$  is shown in (b) for the same  $U = 10$  and two different frequencies above ( $\omega = 16$ , blue solid line) and below ( $\omega = 6$ , red dashed line) the Hubbard gap. Blue dotted and red dash-dotted lines indicate the corresponding perturbative results (Eq. (3)). For large driving strength  $\xi \gtrsim 1$ , a reversal of  $J_{\text{ex}}$  is possible. (c) Illustration of modification of the  $J_{\text{ex}}$  in the Floquet picture by virtual absorption and emission of an arbitrary number of photons.

tain uniform spin resonances that can be conveniently described in mean-field theory. For large dimensions, also a numerical solution of the nonequilibrium electron dynamics in the Hubbard model is possible using the dynamical mean-field theory (DMFT, see Methods).

Within DMFT, the equilibrium solution of the Hubbard model at half-filling and low temperature is the Néel state. In order to assess the exchange interaction in this state, we study the excitation of resonances in the antiferromagnetic phase in a transverse magnetic field  $B_x$ . In equilibrium, the balance of  $B_x$  and  $J_{\text{ex}}$  gives rise to a canting of the magnetic sublattices out of the  $y$ - $z$  plane. If  $J_{\text{ex}}$  is modified under periodic driving, the sublattice magnetizations are no longer aligned with the effective field  $B_{\text{eff}}$  given by external and exchange fields, as illustrated in the inset of Fig. 1. This implies a rotation of the spins in the plane perpendicular to  $B_x$  (leaving the total angular momentum  $S_x$  conserved), from which the time-dependent modification of the exchange interaction is calculated (see Methods).

We have implemented the DMFT solution of the Hubbard model in a time-dependent external electric field for the infinite-dimensional hyper-cubic lattice with density of states  $D(\epsilon) = \exp(-\epsilon^2)/\sqrt{\pi}$  [30, 31]. The electric field is pointing along the body diagonal of the lattice and represents a laser pulse with frequency  $\omega$  and a Gaussian envelope that contains 15 cycles per pulse, *i.e.*,  $E(t) = E_0 \sin(\omega t) \exp(-(t - 3t_c)^2/t_c^2)$  with

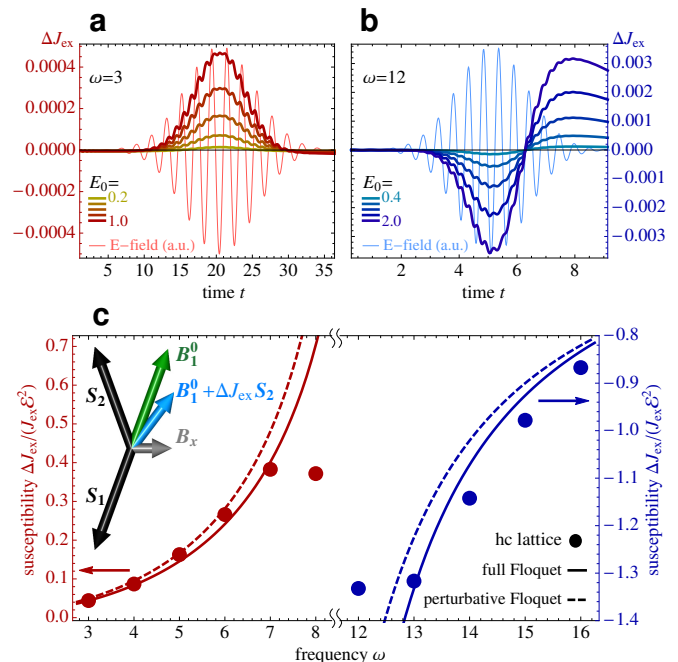


FIG. 2. **Laser-induced modification of the exchange interaction in the Hubbard model on the hyper-cubic lattice.** Panel a and b: Time-dependent change of the exchange interaction ( $\Delta J_{\text{ex}}$ , thick lines) during the action of a laser pulse, for driving frequencies  $\omega = 3$  (a) and  $\omega = 12$  (b) below and above the Mott gap, respectively. Numerical results were obtained using DMFT for the hyper-cubic lattice at  $U = 10$  and initial temperature  $T = 0.025$ . Thin lines show the time dependence of the electric field. c) The driving susceptibility  $\Delta J_{\text{ex}}/(J_{\text{ex}}\mathcal{E}^2)$  for  $\mathcal{E} \rightarrow 0$  for frequencies above (blue, right vertical axis) and below gap (red, left vertical axis), obtained from DMFT for the hc-lattice (disks), from the numerical Floquet spectrum of a two-site Hubbard cluster (solid lines), and from the perturbative result Eq. (3). The inset illustrates the canted geometry of the two sublattice magnetizations  $S_{1,2}$ . Due to a modification of the exchange interaction the direction of the equilibrium mean field  $B_1^0$  is changed, making it no longer collinear with the spin  $S_1$  and causing the excitation of a spin resonance, from which the modification of the exchange interaction is computed (see Methods).

$t_c = 15\pi/(2.1\omega)$ . Fig. 2a and b show time traces of the induced change of the exchange interaction  $\Delta J_{\text{ex}}^c(t)$  for one driving frequency below (a) and above (b) gap, as extracted from the time evolution of the spin degrees of freedom during the pulse. In accordance with the prediction of the Floquet theory we observe an enhancement (reduction) of the exchange interaction during the application of the field with a frequency below (above) gap. The frequency  $\omega = 3$  in Fig. 2a is far from the resonance  $\omega \approx U$ , and we observe that  $\Delta J_{\text{ex}}^c \approx 0$  after the pulse, demonstrating the reversibility of the effect. Conversely, the driving frequency  $\omega = 12$  in Fig. 2b is chosen close to the edge of the upper Hubbard band where we observe significant absorption and transient behavior after the pulse. Hence, although the exchange interaction is mod-

ified in this case as well, the effect is not reversible. Note also that the time reached in the present simulations is too short for the photo-excited carriers to relax, hence a description in terms of a quasi-stationary photo-doped state discussed earlier [15] is not yet valid.

A quantitative comparison with the Floquet theory is shown in the bottom panel of Fig. 2, where the “driving susceptibility”  $\Delta J_{\text{ex}}/(J_{\text{ex}}\mathcal{E}^2)$  for  $\mathcal{E} \rightarrow 0$  is plotted as a function of the driving frequency. Solid discs show the DMFT results as obtained by a linear fit through the dependence of the ratio  $\Delta J_{\text{ex}}(t)/J_{\text{ex}}$  on  $\mathcal{E}^2$  at its maximum. Dashed and solid lines show the results based on the perturbative Floquet formula (Eq. (3)) and the full Floquet spectrum (non-perturbative in  $t_0/U$ ), evaluated from the derivative  $dJ_{\text{ex}}/d\mathcal{E}^2$  at  $\mathcal{E} = 0$ . As expected, in the vicinity of the band edge ( $|\omega - U| \sim 2$ ), strong deviation is found since band absorption is not captured in a cluster picture. Away from the band edge, however, the frequency dependence matches very well, being even in quantitative agreement for the lowest frequencies below gap. This demonstrates the usefulness of the Floquet theory for understanding how off-resonant periodic driving modifies the exchange interaction in extended condensed matter systems by photo-assisted hopping.

**1D quantum spin dynamics** – An intriguing prediction of the Floquet analysis is the existence of amplitude and frequency ranges in which the exchange coupling becomes ferromagnetic (FM). Such a sign change of  $J_{\text{ex}}$  cannot cause a transition to a FM *state* since the Hubbard model Eq. (1) conserves the total spin. However, even if the system remains antiferromagnetic (AFM), a change of sign of  $J_{\text{ex}}$  by periodic driving allows for a very non-trivial and unique way to control the spin dynamics, namely, to *reverse the time evolution* of the undriven system. Such time reversal can be anticipated by considering a pure Heisenberg spin Hamiltonian  $H_{\text{ex}} = J_{\text{ex}} \sum_{\langle ij \rangle} \mathbf{S}_i \mathbf{S}_j$ , which gives an accurate description of the low-energy spin dynamics in the half-filled Hubbard model at  $U \gg t_0$  if the system is not electronically excited. In the absence of driving, the propagation over a time interval  $t$  is given by the evolution operator  $\mathcal{U}_{\text{AFM}} = \exp(-iH_{\text{ex}}t)$ . Such evolution can exactly be reversed by the propagation with an exchange interaction  $J'_{\text{ex}}$  of opposite sign over a time interval  $t' = |J_{\text{ex}}/J'_{\text{ex}}|t$ , since for the FM time evolution operator we have  $\mathcal{U}_{\text{FM}} = \exp(-iH'_{\text{ex}}t') = \exp(+iH_{\text{ex}}t) = \mathcal{U}_{\text{AFM}}^{-1}$ , *i.e.*, the two time evolution operators are exactly inverse to each other.

To demonstrate that periodic driving of the Hubbard model at large  $U$  indeed yields the anticipated time reversal of the spin degrees of freedom, we consider a chain of  $L = 10$  sites and compute the dynamics using exact diagonalization techniques (see Methods). The system is initially prepared in a classical Néel state  $c_{1\uparrow}^\dagger c_{2\downarrow}^\dagger c_{3\uparrow}^\dagger \dots |0\rangle$  and is evolved under the unperturbed Hamiltonian (1). In a quantum Heisenberg model, the classical Néel state is a highly excited state the energy of which exceeds the thermal energy at the Néel temperature, such that no re-

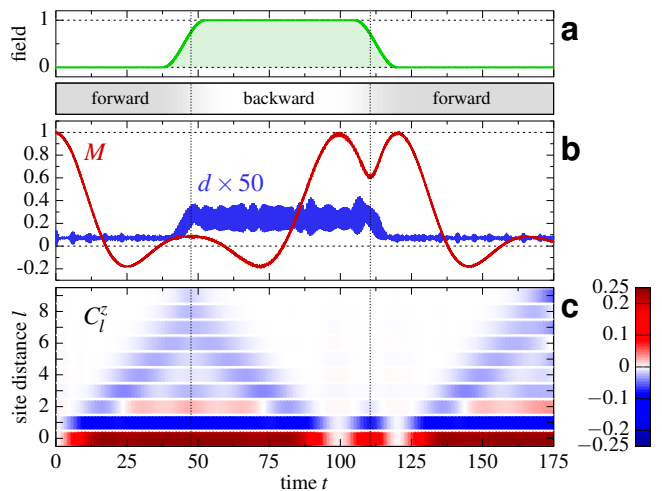


FIG. 3. **Time-reversal of the spin dynamics by periodic driving of a 10-site Hubbard chain.** (a) Field envelope with cosine-shaped ramps of length  $\Delta t = 15$  around  $t_f = 45$  and  $t = 112.5$ . (b) Time evolution of staggered magnetization  $M$  (red) and total double occupation  $d$  (blue), scaled by a factor of 50, showing free evolution for times  $t < 37.5$  and  $t > 120$  and evolution under an additional periodic driving at frequency  $\omega/U = 0.6$  and Floquet amplitude  $\mathcal{E} = 3.4$  in between. (c) Build up and diminishing of the spin-spin correlation function  $C_i^z$ . Numerical results were obtained by exact diagonalization for  $U = 50$  and open boundary conditions, starting from a classical Néel state.

manent long-range order is expected at long times, apart from finite size effects. In one dimension, not even the ground state displays long-range order. As a consequence of the spin-flip terms  $J_{\text{ex}}(S_i^+ S_{i+1}^- + S_i^- S_{i+1}^+)$  in the effective antiferromagnetic Heisenberg model, we thus observe a rapid decay of the total staggered magnetization  $M = \frac{1}{L} \sum_{i=1}^L (-1)^{i+1} \langle n_{i\uparrow} - n_{i\downarrow} \rangle$  (Fig. 3b). After this initial free evolution to a state where long-range order is suppressed, we ramp on a time-periodic electric field (Fig. 3a), with Floquet amplitude  $\mathcal{E} = 3.4$  and frequency  $\omega/U = 0.6$  such that the Floquet theory for a two-site model predicts a reversal of the exchange coupling. Under the periodic driving one indeed observes a near perfect reversal of the dynamics of  $M(t)$  in Fig. 3b, which almost completely recovers to the initial value  $M(t = 0)$  around  $t \approx 100$ . Subsequently,  $M(t)$  is reduced again by further evolution in the reverse direction, as a consequence of the spin-flip terms in the *ferromagnetic* model. This continues until the field is ramped off, after which one observes that the free evolution brings the system again back to the initial state, from which the same rapid decay of  $M(t)$  is observed as for the initial free evolution. Hence, we conclude that the periodic driving allows for a reversible control of the spin dynamics for the timescale considered in our simulations. This is further confirmed by the time evolution of the total double occupation  $d = \sum_{i=1}^L \langle n_{i\uparrow} n_{i\downarrow} \rangle$ , which has the same mean value before and after the driving, demonstrating that

electronic excitations due to the driving are negligible. The weak oscillations in  $d(t)$  are caused by switching on the hopping at  $t = 0$ , while the increased mean value of  $d(t)$  during driving is due to photo-assisted hopping processes.

Time reversal can be demonstrated not only on the level of local observables. Figure 3c displays the evolution of the spin-spin correlation function  $C_l^z = \sum_{|i-j|=l} \frac{1}{N_l} (\langle S_i^z S_j^z \rangle - \langle S_i^z \rangle \langle S_j^z \rangle)$  as a function of distance  $l$  and time ( $N_l$  is the number of site pairs with distance  $l$ ). Starting from the initial uncorrelated product state, correlations build up under the evolution of  $H$ . Even though the system is small, the spreading of correlations resembles the light-cone effect which has been observed in quantum many-body systems after a quench [32], *i.e.*, correlations stay zero outside the light cone  $|l| \leq 2vt$ , where  $v$  is a maximal mode velocity [33], while short-range antiferromagnetic correlations emerge inside the light cone. Further, under the action of the periodic driving, the spin-spin correlations diminish with the same speed, restoring the initially uncorrelated state.

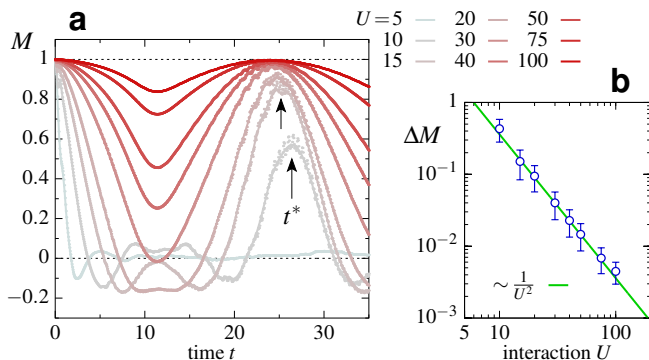


FIG. 4. **Quality of the time reversal.** (a) Time-evolution similar as in Fig. 3 for different values of the interaction  $U$  after fixed forward propagation time  $t_f = 10$ , around which the field is ramped up within a time interval  $\Delta t = 10$ . (b) Difference  $\Delta M$  between the initial magnetization and the magnetization at the revival time  $t^*$  as a function of  $U$ . The amplitude and frequency of the electric field was modeled with the same parameters as used in Fig. 3.

To determine quantitatively how well the time evolution is reversed in our simulations, we computed the difference  $\Delta M = 1 - M(t^*)$  between the initial magnetization in the Néel state and the magnetization  $M(t^*)$  at the revival time  $t^*$  for different values of  $U$  (Fig. 4). In all simulations the system is evolved forward in time for a given time  $t_f = 10$ , after which the field is ramped on for a period  $\Delta t = 10$ . As before we choose  $\mathcal{E} = 3.4$  and  $\omega = 0.6U$ , which gives the same relative change of  $J_{\text{ex}}$  for all sufficiently large values  $U \gg t_0$ . The observed scaling  $\Delta M \sim 1/U^2$  indicates that in the current setup the deviation from perfect reversal originates from small electronic excitations above the gap, which arises from switching on the hopping in the beginning of the simulation and the ramping on of the field. Since the dynamics

of the electronically excited states is not captured by the spin Hamiltonian, it is not time-reversed. While the electronic excitation can be further reduced by slow ramping, the ultimate limit is given by non-Heisenbergian terms in the effective spin Hamiltonian, for which perfect reversal under periodic driving is not expected. For the half-filled Hubbard model in equilibrium, the leading-order correction to the Heisenberg model appears in the order  $t_0^4/U^3$  in the strong-coupling expansion. At least for small times  $t$ , the contribution of a perturbation  $\delta H$  proportional to  $t_0^4/U^3$  to the time-reversed Hamiltonian would lead to a scaling  $\Delta M \sim 1/U^3$ , which is smaller than the electronic excitation in the present case. Note, however, that the times reached in the current simulations are nevertheless long enough to observe near perfect reversal even from a state without magnetic order, in which spin correlations have spread throughout the full chain (Fig. 3).

**Discussion** – Our results demonstrate ultrafast and reversible electrical control of the exchange interaction in extended fermionic many-body systems by modulation with time-periodic electric fields. We emphasize that Floquet amplitudes  $\mathcal{E} \sim 0.1$  are well accessible for condensed matter systems. For example, for a frequency  $\hbar\omega = 1\text{eV}$  and a lattice spacing of  $2\text{\AA}$ , a laser fluence of  $1\text{mJ/cm}^2$  in a 100fs pulse corresponds to a Floquet parameter  $\mathcal{E} = 0.05$ . This is further supported by recently presented experimental results [34], which show the first experimental evidence for optical modification of the super-exchange interaction in canted iron-oxide materials, by off-resonant pumping of charge-transfer transitions. Although our current single-band model is clearly a minimal model in which the modification of the exchange interaction can be studied, it will be very interesting to investigate more complicated exchange models involving multiple bands with various, possibly competing, exchange paths.

In addition, it will be of fundamental interest to investigate the reversal of the exchange interaction and the associated time reversal of the quantum spin dynamics in experiments. Although the large amplitudes  $\mathcal{E}$  needed to realize ferromagnetic exchange at frequencies sufficiently far from resonances  $n\omega = U$  are hard to achieve for most condensed matter systems, a realization of the effect may be possible using cold atoms. In these systems recently great progress has been made to prepare and measure systems with single-site spatial resolution [35, 36]. Cold atoms have been successfully used as a quantum simulator for the dynamics of a quantum quenches in the Bose-Hubbard model, starting from an artificially prepared charge-ordered phase [37], which suggest similar techniques to probe the behavior of spin systems under time reversal. In the methods section (cf. Eq. (7)), we show that analogous time reversal can be achieved by modulating the amplitude of the hopping instead of its phase, which is easier to control in cold atoms. An intriguing problem to study both theoretically and experimentally is the fundamental question how well the time evolution can be reversed after (much) longer forward



evolution time and investigate systematically the influence of small deviations from perfect time-reversal. Furthermore, a study of the Loschmidt echo and dynamical phase transitions [38] in cold atoms might be possible by including additional perturbations to the back propagation.

## II. METHODS

### A. Floquet theory

The Floquet quasi-energy spectrum can be obtained from the ansatz  $|\psi(t)\rangle = e^{-i\epsilon_\alpha t}|\psi_\alpha(t)\rangle$  by expanding  $|\psi_\alpha(t)\rangle$  in a Fourier series  $|\psi_\alpha(t)\rangle = \sum_m e^{i\omega m t}|\psi_{\alpha,m}\rangle$ , where  $|\psi_{\alpha,m}\rangle$  is referred to as the component of the wave function in the  $m$ -th Floquet sector. The Schrödinger equation then achieves a block-matrix structure

$$(\epsilon_\alpha + m\omega)|\psi_{\alpha,m}\rangle = \sum_{m'} H_{m-m'}|\psi_{\alpha,m'}\rangle, \quad (4)$$

where  $H_m = (1/T)\int_0^T dt e^{i\omega m t} H(t)$  are the Fourier components of the Hamiltonian.

Time-dependent electric fields are incorporated into the Hubbard Hamiltonian (1) by adding a time-dependent Peierls phase to the hopping matrix elements,  $t_{ij}(t) = t_0 \exp[ieaA_{ij}(t)]$ , where  $A_{ij}$  is the projection of the vector potential along the direction from site  $i$  to  $j$  (choosing a gauge with zero scalar potential and  $E(t) = -\partial_t A(t)$ ). For the one-dimensional chain with electric field  $E_0 \sin(\omega t)$  along the chain, this implies  $A_{ij}(t) = -\frac{1}{\omega}(i-j)\mathbf{E}_0 \cos(\omega t)$ . The Fourier components of the Hamiltonian are thus given by

$$H_m = -t_0 \sum_{\langle ij \rangle \sigma} (-1)^m J_m((i-j)\mathcal{E}) c_{i\sigma}^\dagger c_{j\sigma}, \quad (5)$$

plus the additional (time-independent) interaction part in the  $m = 0$  component, where  $J_m(x)$  is the  $m$ -th Bessel function, and the dimensionless parameter  $\mathcal{E} = eaE_0/(\hbar\omega)$  measures the strength of the perturbation [cf. Eq. (2)]. For the numerical determination of the Floquet energies, one truncates the number of Floquet sectors in Eq. (4) to  $|n| \leq N$ , and increases  $N$  to reach convergence. The determination of a many-body Floquet spectrum thus requires the diagonalization of a matrix of dimension  $N \times D$  where  $D$  is the dimension of the Hilbert space. The results presented in Fig. 1 are converged with  $N = 8$ .

In the limit of large frequency,  $\omega \gg U, t_0$ , Floquet sectors in Eq. (4) are separated in energy, and one can restrict oneself to the lowest sector  $m = 0$ . This is equivalent to replacing the Hamiltonian with its time average, which leads to the renormalization of the hopping by  $J_0(\mathcal{E})$ , and a corresponding reduction of the exchange by a factor  $J_0(\mathcal{E})^2$ . In the perturbative limit where both  $t_0/U \ll 1$  and  $\mathcal{E} \ll 1$ , we expand the Bessel functions

$J_n(x) \sim x^n$  for  $x \rightarrow 0$ . To lowest order only states of the  $m = 0$  and  $m = \pm 1$  Floquet sectors have to be taken into account, and the result given by Eq. (3) follows from standard second order perturbation theory. Furthermore, an interesting limit for the Mott regime is given by  $t_0/U \ll 1$ , but allowing for fields of arbitrary amplitude. Because all terms  $H_m$  for  $m \neq 0$  are proportional to  $t_0$ , the perturbative shift of the spin states in the  $m = 0$  sector is given by a sum over all second-order processes containing precisely one virtual hopping to a higher Floquet sector and back, yielding

$$\frac{J_{\text{ex}}(\mathcal{E}, \omega)}{J_{\text{ex}}(\mathcal{E} = 0)} = \sum_{n=-\infty}^{\infty} \frac{J_{|n|}(\mathcal{E})^2}{1 + n\omega/U}. \quad (6)$$

The unperturbed exchange is modified by a factor dependent only on  $\omega/U$  and  $\mathcal{E}$ . For the parameters  $\mathcal{E} = 3.4$  and  $\omega/U = 0.6$  chosen for the time reversal, *e.g.*, the factor is given by  $-0.95$  and indicates a near perfect sign reversal.

Finally, we note that a similar analysis is possible for the case of periodic modulation of the hopping amplitude, taking  $t_0(t) = t_0(1 + A \cos(\omega t))$ . As above, we obtain for  $U \ll t$

$$\frac{J_{\text{ex}}(A, \omega)}{J_{\text{ex}}(A = 0)} = 1 + \sum_{n=\pm 1} \frac{A^2}{1 + n\omega/U}, \quad (7)$$

yielding, *e.g.*, a perfect sign reversal for driving above gap  $\omega/U = 1.2$  at  $A \approx 0.67$ . Other than for the field driven case, the perturbation is purely harmonic, and only Floquet sectors  $m = \pm 1$  enter this expression.

### B. Dynamical mean-field theory (DMFT)

To solve the electron dynamics in the Hubbard model we use nonequilibrium DMFT [30, 39]. Within DMFT [40], which becomes exact in the limit of infinite dimensions [41], local correlation functions are obtained from an effective impurity model in which one site of the lattice is coupled to a non-interacting, self-consistently determined bath. A detailed description of the formalism and of our numerical implementation is given in Ref. [15, 30]. The impurity model is solved within the perturbative hybridization expansion (non-crossing approximation, NCA [42]). The accuracy of this approach in the antiferromagnetic and paramagnetic Mott insulator regime  $t_0 \ll U$  has been tested in equilibrium and for short-time dynamics by comparison with higher-order hybridization expansions as well as with numerically exact Quantum Monte Carlo [42–44].

### C. Determination of $J_{\text{ex}}$ in DMFT

In order to assess the exchange interaction from mean-field spin dynamics, we investigate the antiferromagnetic phase of the Hubbard model supplemented with

a term  $B_x \sum_i S_{ix}$ , which couples the spin  $S_{i\alpha} = \frac{1}{2} \sum_{\sigma\sigma'} c_{i\sigma}^\dagger (\hat{\sigma}_\alpha)_{\sigma\sigma'} c_{i\sigma'}$  to a homogeneous magnetic field  $\vec{B}_x$  along the  $x$ -axis ( $\hat{\sigma}_\alpha$  denote the Pauli matrices;  $\alpha = x, y, z$ ). DMFT allows us to compute the time-dependent expectation value of the electron spin  $\langle \mathbf{S}_{1,2} \rangle$  on the two magnetic sublattices. Assuming a rigid macrospin model, the time-dependent exchange interaction can be inferred from these results by inverting the Landau-Lifshitz equation for the dynamics of spins on the mean field  $\mathbf{B}_{\text{eff}}^{1,2} = B_x \mathbf{e}_x - 2J_{\text{ex}} \langle \mathbf{S}_{2,1} \rangle$  [15]. It was shown [15] that this approach compares well to the definition of exchange interactions from a time-dependent response formalism [45], as well as to the analytical perturbative result  $J_{\text{ex}} = 2t_0^2/U$  in equilibrium at large  $U$ . In the transverse field, the equilibrium exchange interaction can be determined from the canting induced by  $B_x$ , yielding  $J_{\text{ex}}^c = -B_x/(4\langle S_x \rangle)$ . Out of equilibrium, we obtain  $J_{\text{ex}}^c(t) = -B_x/(4\langle S_x \rangle) + \Delta J_{\text{ex}}^c(t)$ ,

$$\Delta J_{\text{ex}}^c(t) = -\frac{1}{4T\langle S_{1x} \rangle} \int_{t-T/2}^{t+T/2} \frac{\langle \dot{S}_{1y}(s) \rangle}{\langle S_{1z}(s) \rangle} ds, \quad (8)$$

where the time-averaging is done to extract only the low-frequency component, similar as in the Floquet theory. Note that by calculating the exchange interaction in this way, we have automatically projected out dynamical changes in the (time-averaged) local magnetization  $|\langle \mathbf{S}_{1,2} \rangle|$ , and slight changes of the local moments (double occupation) as a result of the virtual absorption and

emission of photons.

#### D. Exact Diagonalization

To compute the time evolution of the (driven) one-dimensional Hubbard model from the Schrödinger equation with a time-dependent Hamiltonian  $H(t)$  and a given initial state  $|\psi_0\rangle = c_{1\uparrow}^\dagger c_{2\downarrow}^\dagger c_{3\uparrow}^\dagger \dots |0\rangle$  we use the Krylov technique [46] in combination with a commutator-free exponential time-propagation (CFET) scheme [47]. While the Krylov method provides efficient approximations to the time-propagator, which are important to treat large Hilbert spaces, the CFET scheme is related to the Magnus expansion and, preserving unitarity, allows for a high-order accurate integration of the Schrödinger equation in time.

**Acknowledgments** – We thank U. Bovensiepen, M.I. Katsnelson, A.V. Kimel, A. Lichtenstein, R.V. Mikhaylovskiy, T. Oka, A. Secchi, N. Tsuji, and Ph. Werner for fruitful discussions. The exact diagonalization calculations were run in part on the supercomputer HLRN-II of the North-German Supercomputing Alliance. J.H.M. acknowledges funding from the Nederlandse Organisatie voor Wetenschappelijk onderzoek (NWO) by a Rubicon Grant.

- 
- [1] A. Kirilyuk, A. V. Kimel, and T. Rasing, *Rev. Mod. Phys.* **82**, 2731 (2010).
- [2] I. Radu, K. Vahaplar, C. Stamm, T. Kachel, N. Pontius, H. A. Dürr, T. A. Ostler, J. Barker, R. F. L. Evans, R. W. Chantrell, A. Tsukamoto, A. Itoh, A. Kirilyuk, T. Rasing, and A. V. Kimel, *Nature* **472**, 205 (2011).
- [3] J. H. Mentink, J. Hellsvik, D. V. Afanasiev, B. A. Ivanov, A. Kirilyuk, A. V. Kimel, O. Eriksson, M. I. Katsnelson, and T. Rasing, *Phys. Rev. Lett.* **108**, 057202 (2012).
- [4] S. Wienholdt, D. Hinzke, K. Carva, P. M. Oppeneer, and U. Nowak, *Phys. Rev. B* **88**, 020406 (2013).
- [5] V. G. Baryakhtar, V. I. Butrim, and B. A. Ivanov, *JETP Lett.* **98**, 298 (2013).
- [6] R. F. L. Evans, T. A. Ostler, R. W. Chantrell, I. Radu, and T. Rasing, *Applied Physics Letters* **104**, 082410 (2014).
- [7] H.-S. Rhie, H. Dürr, and W. Eberhardt, *Phys. Rev. Lett.* **90**, 247201 (2003).
- [8] G. Ju, J. Hohlfeld, B. Bergman, R. J. M. van de Veerdonk, O. N. Mryasov, J.-Y. Kim, X. Wu, D. Weller, and B. Koopmans, *Phys. Rev. Lett.* **93**, 197403 (2004).
- [9] J. Thiele, M. Buess, and C. H. Back, *Appl. Phys. Lett.* **85**, 2857 (2004).
- [10] S. Wall, D. Prabhakaran, A. T. Boothroyd, and A. Cavalleri, *Phys. Rev. Lett.* **103**, 097402 (2009).
- [11] M. Först, R. I. Tobey, S. Wall, H. Bromberger, V. Khanna, A. L. Cavalleri, Y.-D. Chuang, W. S. Lee, R. Moore, W. F. Schlotter, J. J. Turner, O. Krupin, M. Trigo, H. Zheng, J. F. Mitchell, S. S. Dhesi, J. P. Hill, and A. Cavalleri, *Phys. Rev. B* **84**, 241104 (2011).
- [12] R. Carley, K. Döbrich, B. Frietsch, C. Gahl, M. Teichmann, O. Schwarzkopf, P. Wernet, and M. Weinelt, *Phys. Rev. Lett.* **109**, 057401 (2012).
- [13] T. Li, A. Patz, L. Mouchliadis, J. Yan, T. A. Lograsso, I. Perakis, and J. Wang, *Nature* **496**, 69 (2013).
- [14] M. Matsubara, A. Schroer, A. Schmehl, A. Melville, C. Becher, M. Martinez, D. Schlom, J. Mannhart, J. Kroha, and M. Fiebig, arXiv:1304.2509.
- [15] J. H. Mentink and M. Eckstein, arXiv:1401.5308.
- [16] P. J. Ryan, J. W. Kim, T. Birol, P. Thompson, J. H. Lee, X. Ke, P. S. Normile, E. Karapetrova, P. Schiffer, S. D. Brown, C. J. Fennie, and D. Schlom, *Nat. Commun.* **4**, 1334 (2013).
- [17] D. H. Dunlap and V. M. Kenkre, *Phys. Rev. B* **34**, 3625 (1986).
- [18] F. Grossmann, T. Dittrich, P. Jung, and P. Hänggi, *Phys. Rev. Lett.* **67**, 516 (1991).
- [19] Y.-A. Chen, S. Nascimben, M. Aidelsburger, M. Atala, S. Trotzky, and I. Bloch, *Phys. Rev. Lett.* **107**, 210405 (2011).
- [20] J. L. Lebowitz, *Phys. Today* **46**, 32 (1993).
- [21] A. Polkovnikov, *Ann. Phys.* **326**, 486 (2011).
- [22] T. Caneva, A. Silva, R. Fazio, S. Lloyd, T. Calarco, and S. Montangero, *Phys. Rev. A* **89**, 042322 (2014).
- [23] H. Lignier, C. Sias, D. Ciampini, Y. Singh, A. Zenesini, O. Morsch, and E. Arimondo, *Phys. Rev. Lett.* **99**,

- 220403 (2007).
- [24] T. Oka and H. Aoki, *Phys. Rev. B* **79**, 081406 (2009).
- [25] N. Tsuji, T. Oka, P. Werner, and H. Aoki, *Phys. Rev. Lett.* **106**, 236401 (2011).
- [26] Y. H. Wang, H. Steinberg, P. Jarillo-Herrero, and N. Gedik, *Science* **342**, 453 (2013).
- [27] L. D'Alessio and M. Rigol, arXiv:1402.5141.
- [28] G. Floquet, *Ann. Sci. Ec. Normale Super.* **12**, 47 (1883).
- [29] M. Grifoni and P. Hänggi, *Phys. Rep.* **304**, 229 (1998).
- [30] H. Aoki, N. Tsuji, M. Eckstein, M. Kollar, T. Oka, and P. Werner, *Rev. Mod. Phys.* **86**, 779 (2014).
- [31] V. Turkowski and J. K. Freericks, *Phys. Rev. B* **71**, 085104 (2005).
- [32] M. Cheneau, P. Barmettler, D. Poletti, M. Endres, P. Schausz, T. Fukuhara, C. Gross, I. Bloch, C. Kollath, and S. Kuhr, *Nature* **481**, 484 (2012).
- [33] P. Calabrese and J. Cardy, *Phys. Rev. Lett.* **96**, 136801 (2006).
- [34] A. V. Kimel, PIPT5, Book of Abstracts (2014).
- [35] W. S. Bakr, A. Peng, M. E. Tai, R. Ma, J. Simon, J. I. Gillen, S. Flling, L. Pollet, and M. Greiner, *Science* **329**, 547 (2010).
- [36] M. Endres, M. Cheneau, T. Fukuhara, C. Weitenberg, P. Schau, C. Gross, L. Mazza, M. Bauls, L. Pollet, I. Bloch, and S. Kuhr, *Applied Physics B* **113**, 27 (2013).
- [37] S. Trotzky, Y. A. Chen, A. Flesch, I. P. McCulloch, U. Schollwöck, J. Eisert, and I. Bloch, *Nat. Phys.* **8**, 325 (2012).
- [38] M. Heyl, A. Polkovnikov, and S. Kehrein, *Phys. Rev. Lett.* **110**, 135704 (2013).
- [39] J. K. Freericks, V. M. Turkowski, and V. Zlatić, *Phys. Rev. Lett.* **97**, 266408 (2006).
- [40] A. Georges, G. Kotliar, W. Krauth, and M. J. Rozenberg, *Rev. Mod. Phys.* **68**, 13 (1996).
- [41] W. Metzner and D. Vollhardt, *Phys. Rev. Lett.* **62**, 324 (1989).
- [42] M. Eckstein and P. Werner, *Phys. Rev. B* **82**, 115115 (2010).
- [43] M. Eckstein and P. Werner, *Phys. Rev. Lett.* **110**, 126401 (2013).
- [44] P. Werner, N. Tsuji, and M. Eckstein, *Phys. Rev. B* **86**, 205101 (2012).
- [45] A. Secchi, S. Brener, A. I. Lichtenstein, and M. I. Katsnelson, *Ann. Phys.* **333**, 221 (2013).
- [46] M. Hochbruck and C. Lubich, *SIAM J. Numer. Anal.* **34**, 1911 (1997).
- [47] A. Alvermann and H. Fehske, *J. Comp. Phys.* **230**, 5930 (2011).